ADVANCES IN ATMOSPHERIC SCIENCES, VOL. 33, DECEMBER 2016, 1386–1400

Role of the Oceanic Channel in the Relationships between the Basin/Dipole Mode of SST Anomalies in the Tropical Indian Ocean and ENSO Transition

Xia ZHAO*[1,2], Dongliang YUAN[1,2], Guang YANG[3], Hui ZHOU[1,2], and Jing WANG[1,2]

[1]*Key Laboratory of Ocean Circulation and Waves, and Institute of Oceanology, Chinese Academy of Sciences, Qingdao* 266071*, China*

[2]*Laboratory for Ocean Dynamics and Climate, Qingdao National Laboratory for Marine Science and Technology, Qingdao* 266235*, China*

[3]*Center for Ocean and Climate Research, First Institute of Oceanography, State Oceanic Administration, Qingdao* 266061*, China*

(Received 26 February 2016; revised 24 June 2016; accepted 18 July 2016)

ABSTRACT

The relationships between the tropical Indian Ocean basin (IOB)/dipole (IOD) mode of SST anomalies (SSTAs) and ENSO phase transition during the following year are examined and compared in observations for the period 1958–2008. Both partial correlation analysis and composite analysis show that both the positive (negative) phase of the IOB and IOD (independent of each other) in the tropical Indian Ocean are possible contributors to the El Niño (La Niña) decay and phase transition to La Niña (El Niño) about one year later. However, the influence on ENSO transition induced by the IOB is stronger than that by the IOD. The SSTAs in the equatorial central-eastern Pacific in the coming year originate from subsurface temperature anomalies in the equatorial eastern Indian and western Pacific Ocean, induced by the IOB and IOD through eastward and upward propagation to meet the surface. During this process, however the contribution of the oceanic channel process between the tropical Indian and Pacific oceans is totally different for the IOB and IOD. For the IOD, the influence of the Indonesian Throughflow transport anomalies could propagate to the eastern Pacific to induce the ENSO transition. For the IOB, the impact of the oceanic channel stays and disappears in the western Pacific without propagation to the eastern Pacific.

Key words: Indian Ocean SSTAs, dipole mode, basin mode, ENSO transition, oceanic channel

Citation: Zhao, X., D. L. Yuan, G. Yang, H. Zhou, and J. Wang, 2016: Role of the oceanic channel in the relationships between the basin/dipole mode of SST anomalies in the tropical Indian Ocean and ENSO transition. *Adv. Atmos. Sci.*, **33**(12), 1386–1400, doi: 10.1007/s00376-016-6048-4.

1. Introduction

ENSO is the most pronounced interannual variability in the tropics, contributing significantly to climate fluctuations in many regions of the globe. Several causal mechanisms of ENSO oscillation have been suggested, such as the delay oscillator (Suarez and Schopf, 1988), the recharge oscillator (Jin, 1997a, 1997b), and the Western Pacific Oscillator (Weisberg and Wang, 1997). These mechanisms emphasize processes in the Pacific Ocean basin, but they do not consider the cross-basin linkage between the tropical Pacific and Indian oceans. The Indian Ocean's variability may affect that in the Pacific Ocean, although most attention has been paid to the impact of the Pacific on the Indian Ocean (e.g., Ding and Li, 2012). There is evidence that SST variability in the Indian Ocean can modulate ENSO variability either through atmospheric wind variability (Yasunari, 1985, 1987; Yu et al., 2002; Behera and Yamagata, 2003; Wu and Kirtman, 2004; Kug and Kang, 2006; McPhaden, 2008; Xie et al., 2009; Izumo et al., 2010; Luo et al., 2010; Du et al., 2013) or Indonesian Throughflow (ITF) variability (Wyrtki, 1987; Wajsowicz and Schneider, 2001; Yuan et al., 2011, 2013). This provides hope for enhanced ENSO prediction skill (Izumo et al., 2010; Luo et al., 2010).

It is well known that the SST anomalies (SSTAs) in the tropical Indian Ocean often co-occur with ENSO variation. Thus, studies tend to focus on the synchronous influence of the Indian Ocean on the Pacific (e.g., Annamalai et al., 2005, 2010). On the other hand, several studies have provided evidence that the Indian Ocean acts as a negative feedback mechanism to ENSO (Kug and Kang, 2006; Kug et al., 2006; Ohba and Ueda, 2007; Izumo et al., 2010; Yuan et al., 2011, 2013; Zhou et al., 2015). The suggestion is that the Indian Ocean SSTAs during El Niño (La Niña) lead to a relatively faster ENSO termination and phase transition to La Niña (El Niño). Such a lagged impact of the tropical Indian Ocean on the Pacific is the focus of the present paper.

The most dominant SST variations in the tropical Indian Ocean are the basin-wide warming/cooling mode (hereafter,

* Corresponding author: Xia ZHAO
Email: zhaoxia@qdio.ac.cn

the IOB) (e.g., Yang et al., 2007) and the dipole mode (hereafter, the IOD) (Saji et al., 1999; Webster et al., 1999), which can be obtained via EOF analysis of the tropical Indian Ocean SST variability, i.e., EOF-1 and EOF-2, respectively (Fig. 1). The IOB involves a near uniform warming (cooling) over the entire basin. It reaches its maximum after the mature phase of ENSO. The IOD involves a weak warming (cooling) over the western Indian Ocean and a strong cooling (warming) in the east off Java and Sumatra (Saji et al., 1999; Webster et al., 1999). The IOD peaks in fall then quickly recedes. Results show that much of the IOB is caused by ENSO-induced surface heat flux anomalies (Klein et al., 1999). However, there are different views regarding the IOD, with some suggesting it is independent of ENSO (e.g., Saji and Yamagata, 2003; Yamagata et al., 2003) and others indicating it to be primarily forced by ENSO (Xie et al., 2002; Annamalai et al., 2005; Ohba and Ueda, 2005). Regardless of the origins of the IOB and IOD, they significantly affect ENSO evolution or transition when the Indian Ocean SSTAs appear.

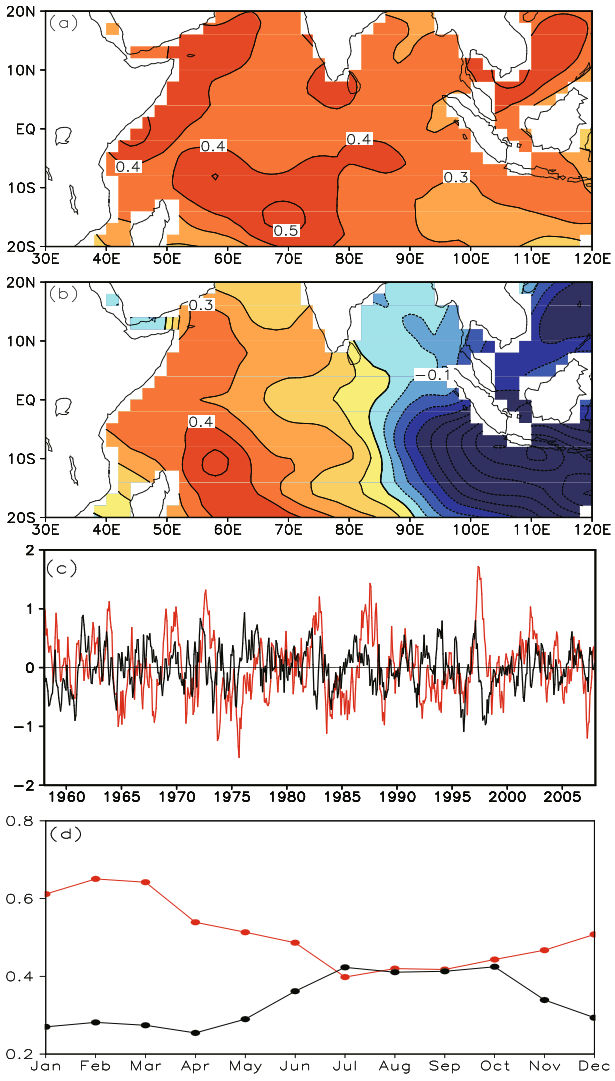

Fig. 1. The (a) first and (b) second EOF modes, with (c) their PCs, of the monthly SSTAs in the tropical Indian Ocean, from the ERSST data for the period 1958–2008. (d) Standard deviation of the PC of the first mode (PC1) and the PC of the second mode (PC2) as a function of calendar month. The red (black) curves in (c) and (d) denote PC1 (PC2).

For the IOD, Izumo et al. (2010) and Yuan et al. (2011, 2013) investigated its influence on the following year's El Niño, and they indicated that a positive (negative) phase of the IOD tends to co-occur with El Niño (La Niña) and favors La Niña (El Niño) about 1 year later. The former study concentrated on the impact of the atmospheric bridge between the Indian and Pacific oceans over the period 1981–2009. On the other hand, Yuan et al. (2011, 2013) focused on the oceanic channel and assigned a key role to the ITF for the period 1990–2009. The positive (negative) phase of the IOD is accompanied by a negative (positive) SSH anomalies (SSHAs) in the tropical eastern Indian Ocean, which forces upwelling (downwelling) Kelvin waves at the equator. The upwelling anomalies propagate eastward from the Indian Ocean into the western equatorial Pacific Ocean through the channels of the seas of Indonesia. They force an enhanced (weakened) ITF to transport more (less) warm water from the upper-equatorial Pacific Ocean to the Indian Ocean. This anomalous transport produces thermocline depth anomalies and cold (warm) subsurface temperature anomalies in the western equatorial Pacific Ocean. Then, these temperature anomalies propagate to the eastern equatorial Pacific, inducing a La Niña (El Niño) in the following year. Thus, their observational and numerical modeling results suggested that the ITF plays an important role in propagating the Indian Ocean anomalies into the equatorial Pacific Ocean, and this ocean channel between the two basins is important for the evolution and predictability of ENSO.

For the IOB, Kug and Kang (2006) and Kug et al. (2006) revealed that positive phases tend to favor phase transition of El Niño to La Niña through anomalous easterly in the western Pacific, paying attention to the atmospheric teleconnection over the period 1958–2000. However, it is unclear whether the modulation of the oceanic channel between the Indian and Pacific oceans plays a role in the relationship between Indian Ocean SSTAs and ENSO transition.

As reviewed above, the relationships between the IOB/IOD over the tropical Indian Ocean and ENSO evolution have previously been examined somewhat in isolation and through using data with different time periods. We note that the impacts of the IOB and IOD have not been discussed and compared together through observational diagnostics. In particular, IOD events are always followed by IOB events, but previous studies do not consider the effect between these two modes. Moreover, numerical simulations are inconsistent with observational results. For instance, using a CGCM, Ohba and Ueda (2007) indicated that during boreal winter the IOB enhances surface easterlies over the equatorial western Pacific during the mature-decay phase of El Niño, which induces a transition to a La Niña phase through upwelling Kelvin waves. However, their model experiment did not reproduce the significant impact of the IOD on the Pacific. Thus, the first purpose of the present paper is to compare the

relationships between the IOB/IOD and ENSO phase transition using observational data, after excluding the effect of the preceding IOD and following IOB through partial correlation analysis and composite analysis. In addition, for the IOB, previous studies focused only on the atmospheric bridge process, neglecting the role of the oceanic channel process in the relationships with ENSO transition. Therefore, the second purpose of the present paper is to discuss whether the relative role of the oceanic channel is similar for these two leading SSTAs modes.

The present study investigates the impact of the external forcing of the tropical Indian Ocean on the Pacific. We attempt to reveal and compare the relationships between the two major SSTAs patterns in the tropical Indian Ocean and the decay and phase transition of ENSO in the following year using observational data from 1958 to 2008, as well as discuss the dynamics associated with the oceanic channel, especially after separating the effect of the IOD and IOB. Our comparison of the impacts of the IOB and IOD will provide a more comprehensive understanding of the role of the Indian Ocean in ENSO variability, and confirm previous model results. Note that the present paper is not to discuss whether or not ENSO triggers the SSTAs in the tropical Indian Ocean. We only study the impacts of the Indian Ocean on the Pacific, and consider how they influence ENSO decay and transition in the following year when the Indian Ocean SSTAs patterns appear.

2. Data

The latest version of ERSST, i.e., ERSST.v3b, is obtained from http://www.esrl.noaa.gov/psd/. The field is on a $2^\circ \times 2^\circ$ global latitude–longitude grid (Xue et al., 2003; Smith et al., 2008). The other SST data used in this study are from the HADISST dataset (Rayner et al., 2003), compiled on a $1^\circ \times 1^\circ$ latitude–longitude grid.

The subsurface temperature, salinity, sea level and horizontal velocity data are obtained from the monthly means of the SODA (version 2.1.6) product for 1958–2008 (Carton and Giese, 2008). This dataset is available at a $0.5^\circ \times 0.5^\circ$ horizontal resolution and has 40 vertical levels with 10-m spacing near the surface. Xie et al. (2002) indicated that SODA agrees well with expendable bathythermograph data; plus, many previous studies have used SODA data to calculate ITF transport (e.g., England and Huang, 2005; Potemra, 2005; Tillinger and Gordon, 2009). Another reanalysis dataset used is the ECMWF's ORAS4 (Ocean Reanalysis System 4). These data (Mogensen et al., 2012; Balmaseda et al., 2013) are available at a horizontal resolution of $1^\circ \times 1^\circ$, with 42 vertical levels and an approximate 10-m level thickness in the upper 200 m. Compared with conventional observational datasets, these two reanalysis datasets provide a longer time record (1958–2008) to investigate the relationship between the ITF and Indo-Pacific variability on the interannual to decadal timescales.

The analysis period for this study is 51 years, from January 1958 to December 2008, because the SODA data are only available from 1958 to 2008. The annual cycle of each variable is removed by subtracting the monthly mean at each grid point. And the anomalies used in the present paper are detrended after removing the annual cycle.

3. Results

3.1. *Relationships between the IOB/IOD and ENSO transition*

The IOB and IOD over the tropical Indian Ocean are derived from EOF-1 and EOF-2 of the ERSST data, respectively (Figs. 1a and 1b). EOF-1 and EOF-2 account for 32% and 14% of the total variance, respectively. Note that the anomalies used in this study are detrended after removing the annual cycle. Through analyzing the principal component (PC) of EOF (Fig. 1c), it can be seen that the seasonal variability of the IOB (PC1) and IOD (PC2) has an obvious phase-locking feature (Fig. 1d). The IOB is strongest in boreal winter (February to March). The maximum of the IOD occurs in fall (July to October) in the ERSST data, which shows a maximum in September to October in the HADISST data (not shown). In order to investigate the influences of the IOB and IOD on the temporal evolution of ENSO, PC1 during February–March is chosen to define the boreal winter IOB index (WBI), and we use PC2 during September–October as the boreal fall IOD index (FDI). Note that different months are used to accord the seasonal dependence of the IOB and IOD. Moreover, the following results associated with the WBI and FDI are not sensitive to the months used for the definition of these two indexes. PC1 (PC2) during January–March (August–October) shows similar results.

We denote the ENSO-developing year as year 0, the decaying year as year 1, and the following year as year 2. The top panels of Fig. 2 give the lagged correlations between the WBI/FDI and the equatorial (2°S–2°N) SSTAs from September (year 0) to June (year 2) using the ERSST dataset. The longitude–time sections of the lagged correlation are used to describe the influence of the IOB and IOD in the tropical Indian Ocean on the temporal evolution of ENSO, separately. It can be seen that the WBI is closely correlated with the following equatorial eastern Pacific SSTAs. In boreal winter (year 0), the correlation is positive in the Indian Ocean, showing the effect of a positive IOB during the peak phase. In addition, positive correlation in the equatorial eastern Pacific indicates that a positive IOB tends to co-occur with El Niño. In the following spring to summer (year 1), the positive correlation in the Indian Ocean begins to weaken, which means that the IOB decays. In the meantime, the positive correlation in the equatorial eastern Pacific diminishes and rapidly changes to an opposite sign, suggesting that a positive IOB of the Indian Ocean leads to a relatively faster termination of El Niño and phase transition. The La Niña then begins from July (year 1) and persists until the next year's spring. The situation is similar for the FDI, except for a negative correlation over the eastern Indian Ocean and western Pacific Ocean

during the first winter (year 0), showing the effect of a peak positive IOD phase. For negative phases of the IOB and IOD, the conditions are the same but with anomalies of opposite sign. The relationship between the WBI/FDI and ENSO evolution is also obtained from the HADISST dataset. The above results show that both the IOB and IOD in the tropical Indian Ocean possibly feed back negatively on ENSO evolution.

Because IOD events are always followed by IOB events, one may imagine that the correlation between the tropical Indian SSTAs and the ENSO phase transition during the following year is induced only by the IOD. Furthermore, we use partial correlation (Cohen and Cohen, 1983) to remove the partial influence of the preceding IOD and following IOB, respectively. This method has been used in many previous studies (e.g., Saji and Yamagata, 2003; Yu et al., 2005; Kug and Kang, 2006; Izumo et al., 2014). As shown in the bottom panels of Fig. 2, in the following year, the significant negative lag correlations in the equatorial central-eastern Pacific still exist for both the IOB and IOD after excluding each other's effects. Therefore, the lagged teleconnection between the IOB/IOD and ENSO transition is not interdependent. Compared to the IOB, however, the negative lagged correlation in the equatorial eastern Pacific during summer to winter (year 1) is obviously weaker for the IOD.

One may doubt that the above lagged correlation may not imply a cause–effect relationship. To clarify this problem, composite analysis is further conducted. Figure 3 shows the time series of the WBI, FDI and Niño3.4 SSTAs during December–February. The Niño3.4 SSTAs are averaged over (5°S–5°N, 170°–120°W). It can be seen that some positive (negative) IOB and IOD events concur with El Niño (La Niña) events. In addition, in the following year, the tropi-

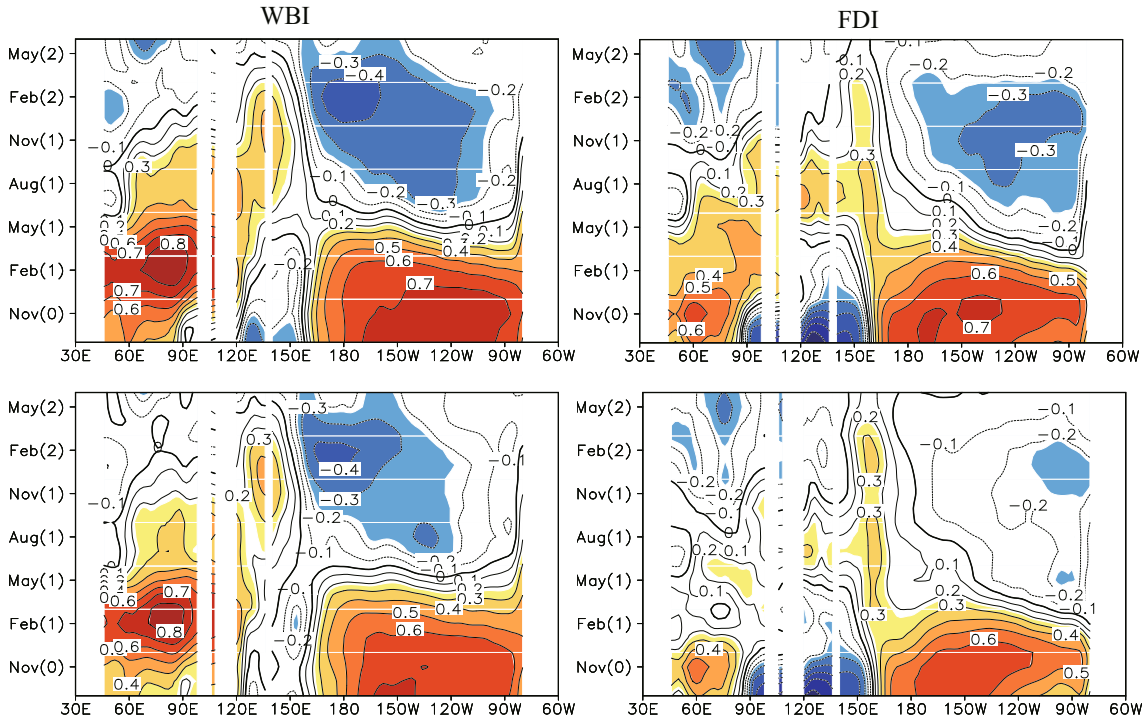

Fig. 2. Left-hand panels: lagged correlations between the WBI and equatorial SSTAs (2°S–2°N) from September (year 0) to June (year 2). Right panels: lagged correlations between the FDI and equatorial SSTAs. In the bottom panels the partial influence of the IOD (left-hand panel) and IOB (right-hand panel) on the equatorial SSTAs is removed using the partial correlation. The color shading indicates positive (warm color) and negative correlations (cold color) above the 90% significance level.

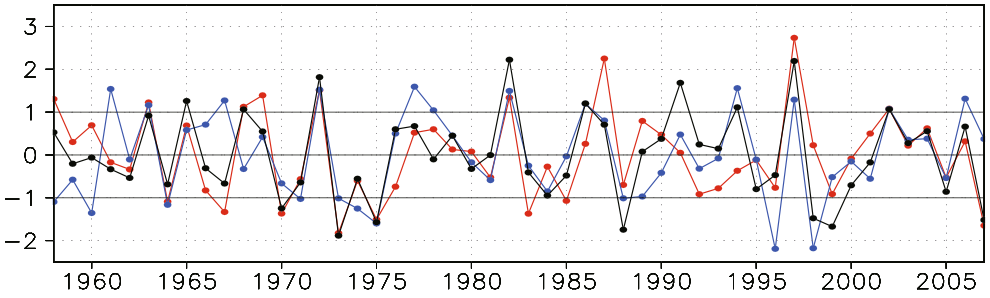

Fig. 3. Time series of the WBI (red), FDI (blue) and Niño3.4 SSTAs during December–February (black).

cal Pacific is mostly in its cold (warm) phase. Similarly, it is necessary to separate the effect of the IOD and IOB due to some of IOD events coinciding with IOB events. Ultimately, eight independent IOB events over the period 1958–2008, each greater than one standard deviation and not coincident with IOB events (positive events: 1958, 1968, 1969, 1987; negative events: 1967, 1970, 1983, 1985), are chosen to carry out the composite analysis. For the composite IOD, there are 14 independent events greater than one standard deviation and not coincident with IOB events (positive events: 1961, 1967, 1977, 1978, 1986, 1994, 2006; negative events: 1958, 1960, 1971, 1974, 1988, 1996, 1998).

Figure 4 shows the composites of the tropical SSTAs for the difference between independent positive and negative IOB events (left panels) and the difference between independent positive and negative IOD events (right panels) from the boreal fall (year 0) season [SON(0), September–November(0)] through the spring (year 2) season [MAM(2), March–May(2)]. For the IOB (left panels of Fig. 4), the SSTAs are positive in the Indian Ocean in the winter (year 0) [D(0)JF(1), December(0)–February(1)], which is accompanied by warming in the central-eastern Pacific. However, the

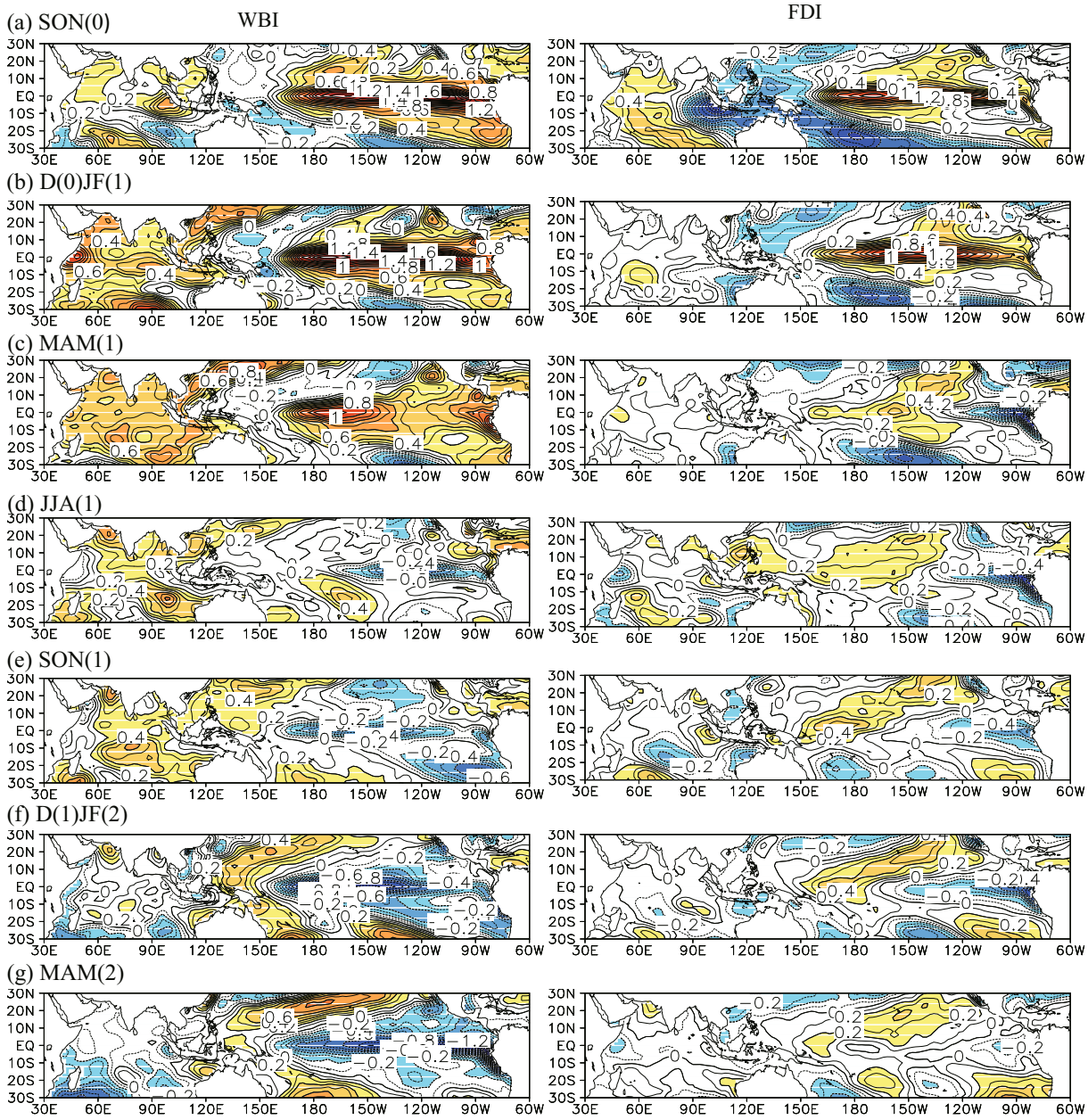

Fig. 4. Composites of tropical SSTAs for the difference between independent positive and negative IOB events (left-hand panels) and the difference between independent positive and negative IOD events (right-hand panels) in different seasons over the period 1958–2008: (a) fall (year 0) [SON(0)]; (b) winter (year 0) [D(0)JF(1)]; (c) spring (year 1) [MAM(1)]; (d) summer (year 1) [JJA(1)]; (e) fall (year 1) [SON(1)]; (f) winter (year 1) [D(1)JF(2)]; and (g) spring (year 2) [MAM(2)]. Color shading indicates that the positive (negative) SSTAs (°C) greater (less) than 0.2.

positive SSTAs in the central-eastern Pacific become weak in the coming spring (year 1) [MAM(1), March–May(1)] and changes to negative in the following summer (year 1) [JJA(1), June–August(1)]. These negative SSTAs develop in the following fall (year 1) and winter (year 1) seasons. For the IOD (right panels of Fig. 4), the SSTAs are negative in the tropical eastern Indian Ocean and positive in the western and central Indian Ocean in the late fall (year 0), which reflects the impact of the peak positive IOD phase. At the same time, a significant teleconnection is demonstrated by the positive SSTAs in the eastern Pacific and the negative values in the western Pacific. The SSTAs over the equatorial central-eastern Pacific change to an opposite sign in the following spring and persists in the following summer to winter seasons. The SSTA's evolution shows some differences between the IOB and IOD. The anomalies in the central-eastern Pacific during the second year induced by the IOB are obviously stronger than those induced by the IOD, and the former is located in the equatorial central-eastern Pacific while the latter is situated in the eastern Pacific. Thus, similar to the result of the lagged correlation analysis, composite analysis supports our conclusion.

In previous studies, the relationships between the IOB/IOD and ENSO evolution have been examined in isolation. In particular, the effect between these two modes has not been considered. Moreover, the model experiment of Ohba and Ueda (2007) did not reproduce this significant connection between the IOD and the tropical central-eastern Pacific. Our result, using partial correlation and composite analysis and the same data, indicates that both the IOB and IOD could lead to ENSO phase transition. The difference is that the influence induced by the IOB is stronger than that by the IOD.

3.2. *The relative role of the oceanic channel*

Izumo et al. (2014) indicated that a positive IOD in fall and a positive IOB in winter both promote a transition of ENSO events during the coming year, through the wind anomalies over the western Pacific promoted by both IOD and IOB events (e.g., Kug and Kang, 2006; Ohba and Ueda, 2007). In addition to the atmospheric bridge, some studies have indicated an influence of the tropical Indian on ENSO transition through modulation of the ITF (Sprintall et al., 2000; Wijffels and Meyers, 2004; Kandaga et al., 2009; Drushka et al., 2010; Yuan et al., 2011, 2013). Yuan et al. (2011, 2013) suggested that the IOD could induce ENSO phase transition through transport variations of the ITF, using observational data and numerical experiments. However, the role of the ITF in the relationship between the IOB and SSTAs evolution in the equatorial Pacific has not been discussed. Therefore, it is necessary to compare the relative roles of the oceanic channel process in the relationship between the IOB/IOD and ENSO evolution in the following year.

From the above analysis in section 3.1, it can be seen that the SSTAs in the equatorial central-eastern Pacific about 1 year later do not come from the horizontal propagation of the SST signal elsewhere. For the IOD, Yuan et al. (2013) indicated that lagged correlations in the subsurface temperature in a vertical section of the equatorial Pacific Ocean suggest eastward propagation of the upwelling anomalies from the Indian Ocean into the equatorial Pacific Ocean through the seas of Indonesia. This result seems to suggest that the ocean channel connection between the two basins is important for the evolution and predictability of ENSO. Following the work of Yuan et al. (2013), Fig. 5 shows the partial correlations between the WBI (FDI) and subsurface temperature anomalies in a vertical section of the equatorial Indian and Pacific oceans from the SODA data, in which the partial influence of the IOD (IOB) on the equatorial SSTAs is removed using the partial correlation. Similar to the result of the IOD (right-hand panels), for the IOB (left-hand panels) the cold SSTAs in the equatorial central-eastern Pacific in the following year come from cold subsurface temperature anomalies in the equatorial eastern Indian and western Pacific oceans, which propagate eastward and upward along the thermocline to arrive at the surface. The result from the ECMWF ORAS4 data (not shown) is consistent with that of the SODA data. Furthermore, composites of tropical subsurface temperature anomalies for the difference between independent positive and negative IOB (IOD) events also support the result of the partial correlation analysis (Fig. 6).

However, Kug and Kang (2006) and Ohba and Ueda (2007) indicated that the generation and propagation of subsurface temperature anomalies in the Pacific possibly comes from the atmospheric bridge process associated with the IOB/IOD. Anomalous easterlies (westerlies) in the equatorial western Pacific during the mature phase of El Niño (La Niña), exciting the equatorial oceanic Kelvin wave, plays a role in ENSO transition. Therefore, in addition to the oceanic channel, Figs. 5 and 6 also include the effect of the atmospheric bridge process related to the IOB/IOD. It is necessary to clarify the relative role of the oceanic channel process in the relationship between the IOB/IOD and ENSO transition.

Figure 7 shows the time series of the monthly transport anomalies of the ITF dealing with the low-pass-filter. The anomalies of the ITF volume transport are defined as the depth-integrated northward velocity in reference to the 729-m level of no motion through a zonal chokepoint section at 8.25°S, based on the SODA data. The time series are filtered by a Gaussian filter using a cutoff period at 13 months. Negative values indicate transports from the Pacific to the Indian Ocean. England and Huang (2004) suggested that the ITF from the SODA reanalysis data is a reasonably accurate reconstruction of the observed ITF, and the ITF transport anomalies derived from the geostrophic flow show broadly similar behavior. The ECMWF ORAS4 data show a similar temporal evolution.

Figure 8 shows the lagged correlations between the ITF transport anomalies during the peak phase of the IOB/IOD and subsurface temperature anomalies in the equatorial Indian and Pacific vertical section during the following seasons from the SODA data. Clearly, for the IOD (right-hand panels), the cold subsurface temperature anomalies in the eastern Indian Ocean and western Pacific Ocean, associated with

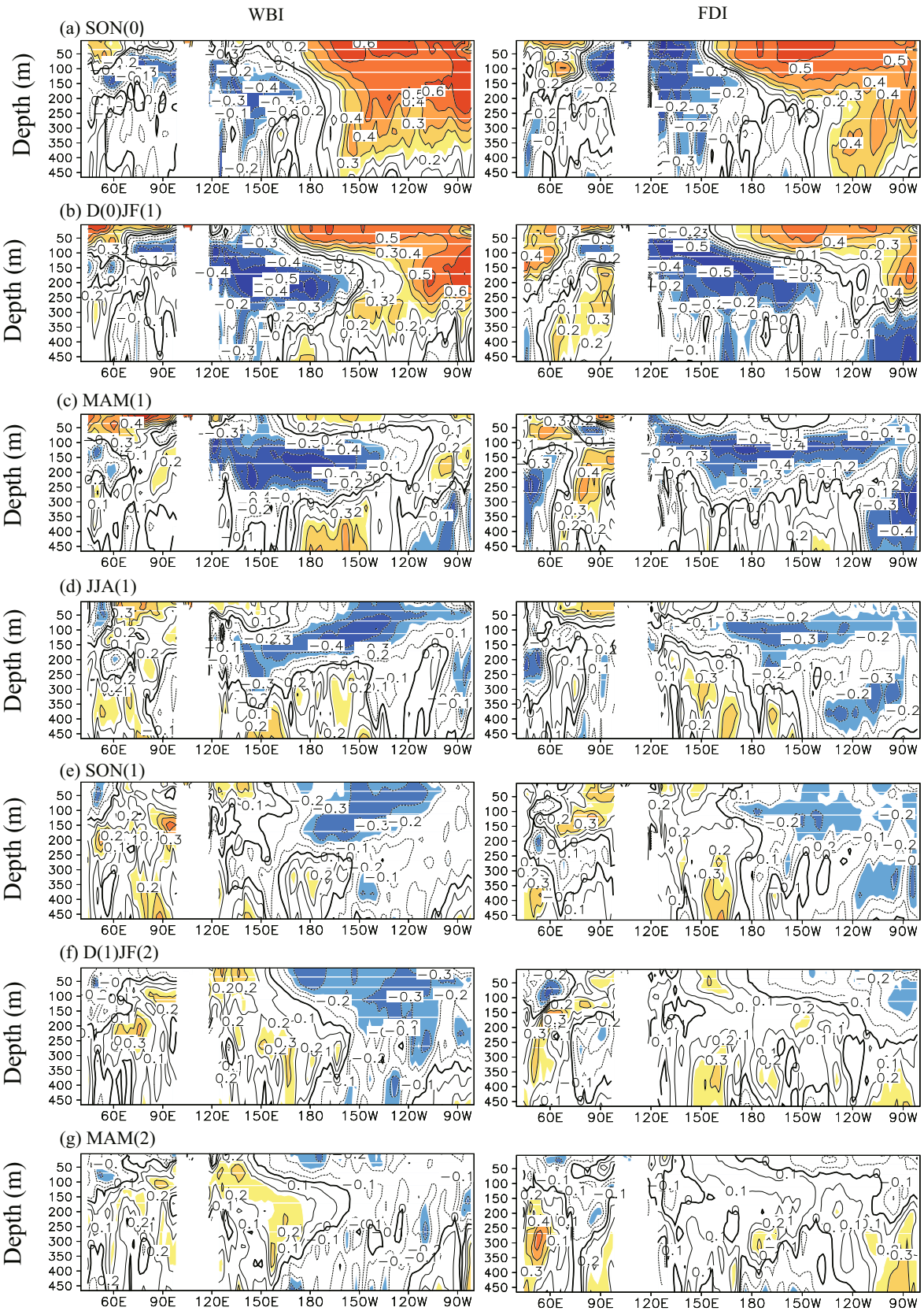

Fig. 5. Left-hand panels: partial correlations between the WBI and subsurface temperature anomalies in the Indian–Pacific equatorial vertical section from SODA data in different seasons, in which the partial influence of the IOD on the equatorial SSTAs is removed using the partial correlation. Right-hand panels: as in the left-hand panels, but for the FDI, in which the partial influence of the IOB is removed. Color shading indicates positive and negative correlations above the 90% significance level.

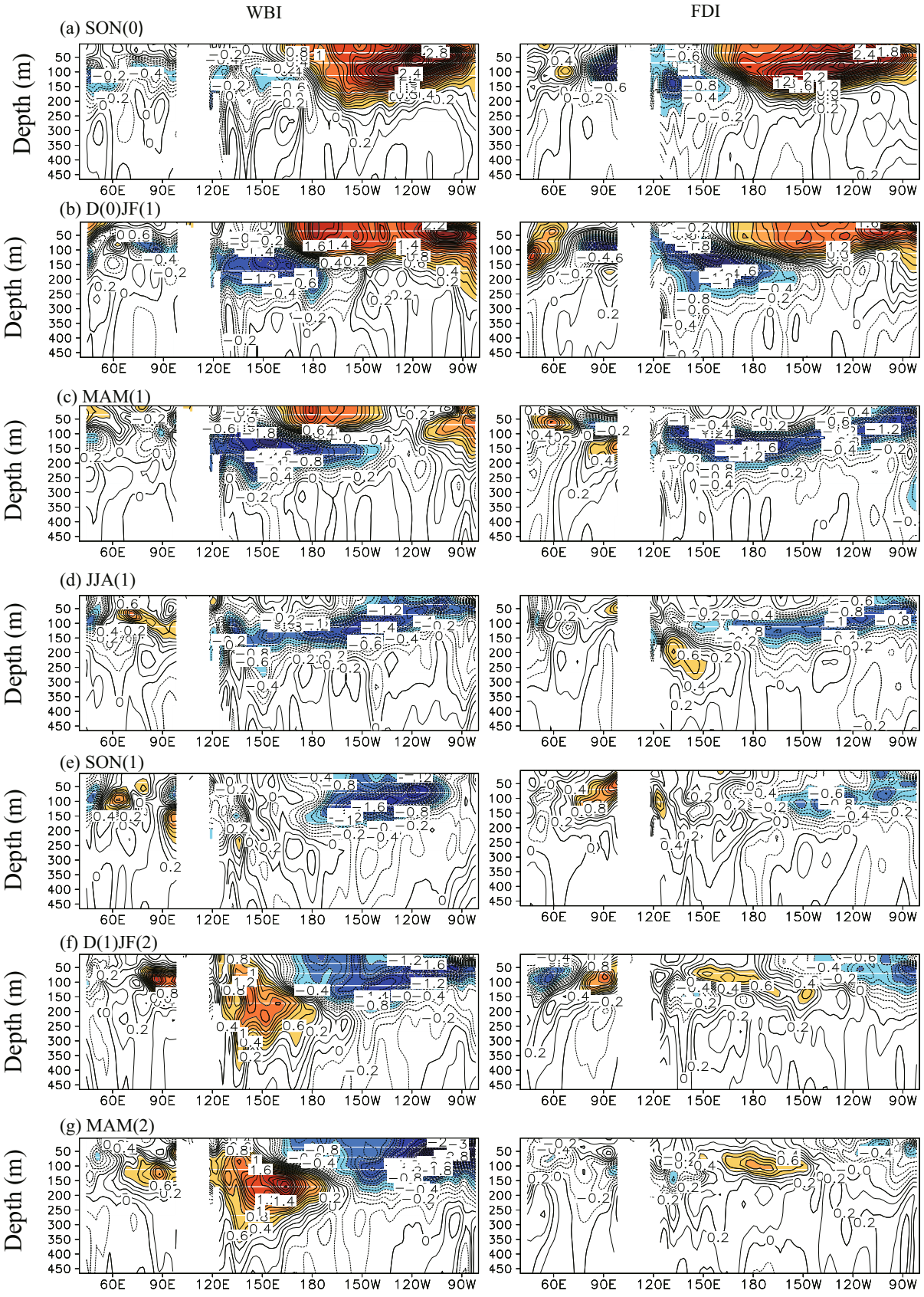

Fig. 6. Composites of tropical subsurface temperature anomalies (°C) in the Indian–Pacific equatorial vertical section from the SODA data for the difference between independent positive and negative IOB events (left-hand panels) and the difference between independent positive and negative IOD events (right-hand panels). Color shading indicates that the positive (negative) subsurface temperature anomalies greater (less) than 0.5.

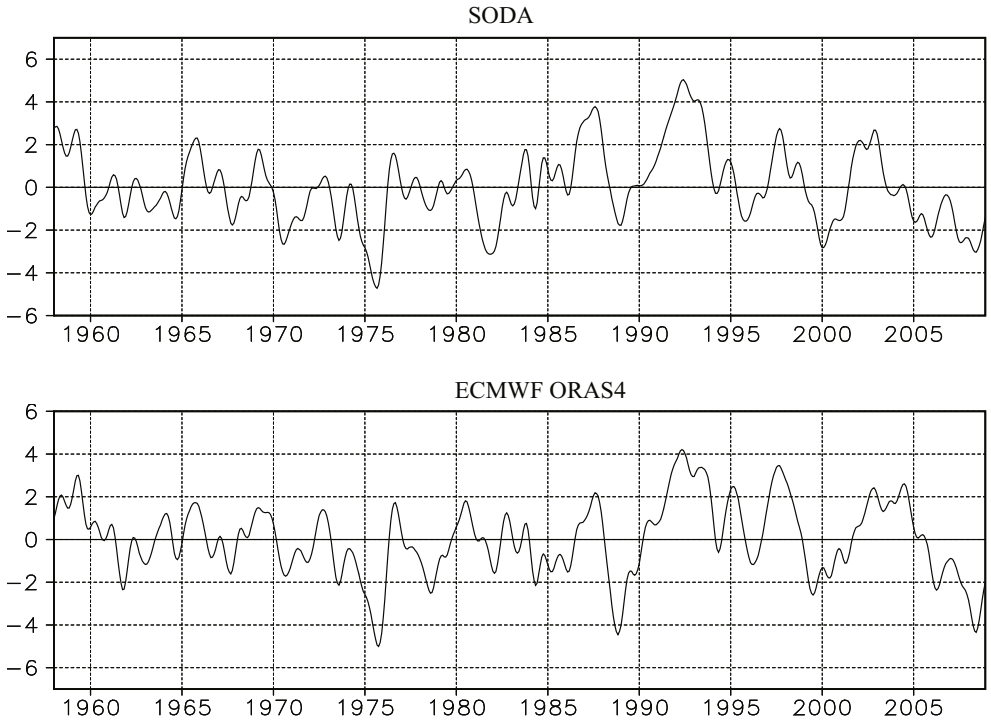

Fig. 7. Low-pass-filtered time series of the monthly ITF transport anomalies from the SODA data (top panel) and ECMWF ORAS4 data (bottom panel).

the ITF transports anomalies, could propagate eastward and upward along the thermocline to arrive at the surface in the central-eastern Pacific during the following winter (year 1). For the IOB (left-hand panels), however, the negative anomalies only stay in the tropical western Pacific and the seas of Indonesia in winter (year 0), which weakens in the following summer and disappears in the following fall (year 1). The ITF transport anomalies during the peak phase of the IOB are not significantly correlated with subsurface temperature anomalies in the central-eastern Pacific in the following summer (year 1) to winter (year 1). Thus, the ITF transport anomalies related to the IOD might induce the SSHAs and SSTAs in the central-eastern Pacific during the following seasons through the eastward propagation of upwelling Kelvin waves. However, the ITF influence induced by the IOB only stays and disappears in the tropical western Pacific without propagation to the equatorial eastern Pacific to affect the temperature in the cold tongue. The result from the ECMWF ORAS4 data is consistent with that of the SODA data (not shown).

To clearly show the contribution of the ITF transport anomalies induced by the IOB/IOD on ENSO phase transition, we repeat the composites of tropical subsurface temperature anomalies in Fig. 6 after removing the influence of ITF transport anomalies during the peak phase of the IOD/IOB (Fig. 9). For the IOB (left-hand panels), the influence of the ITF anomalies on the equatorial Pacific subsurface temperature is very small, because the Pacific subsurface temperature anomalies still have similar values after removing the ITF signal. For the IOD (right-hand panels), the negative subsurface temperature anomalies are weakened in the equatorial Pacific in the following seasons, especially in the eastern Pacific, after the removal of the ITF signal induced by the IOD. This suggests that the oceanic channel between the tropical Indian and Pacific oceans contributes to the dynamics of the lagged teleconnection between the IOD and the ENSO evolution in the following year, but the ITF transport anomalies is ineffective as a link between the IOB signals and ENSO phase transition.

4. Discussion

This paper only investigates the impact of external forcing from the tropical Indian Ocean. The internal dynamics over the tropical Pacific is still vital during ENSO evolution. The external forcing from the Indian Ocean may reinforce local processes in the Pacific, which could affect ENSO evolution in the coming year. It is well known that ENSO has a typical period of roughly 3–7 years and a biennial (~2 yr) component. However, the quasi-biennial oscillation is not strong. Although lagged correlations between the Nino3.4 SSTAs index during the mature phase of ENSO and the equatorial Pacific SSTAs reverse to being negative during the following summer (year 1) to winter (year 1), the negative values are not significant (not shown). However, because of the influence of the tropical Indian Ocean, the ENSO phase reversal seems to complete in one year after the mature phase of ENSO (Fig. 2). This suggests that the ENSO cycle shows enhanced variability for periods of about 2 years. Also, previous modeling studies indicate that ENSO's biennial com-

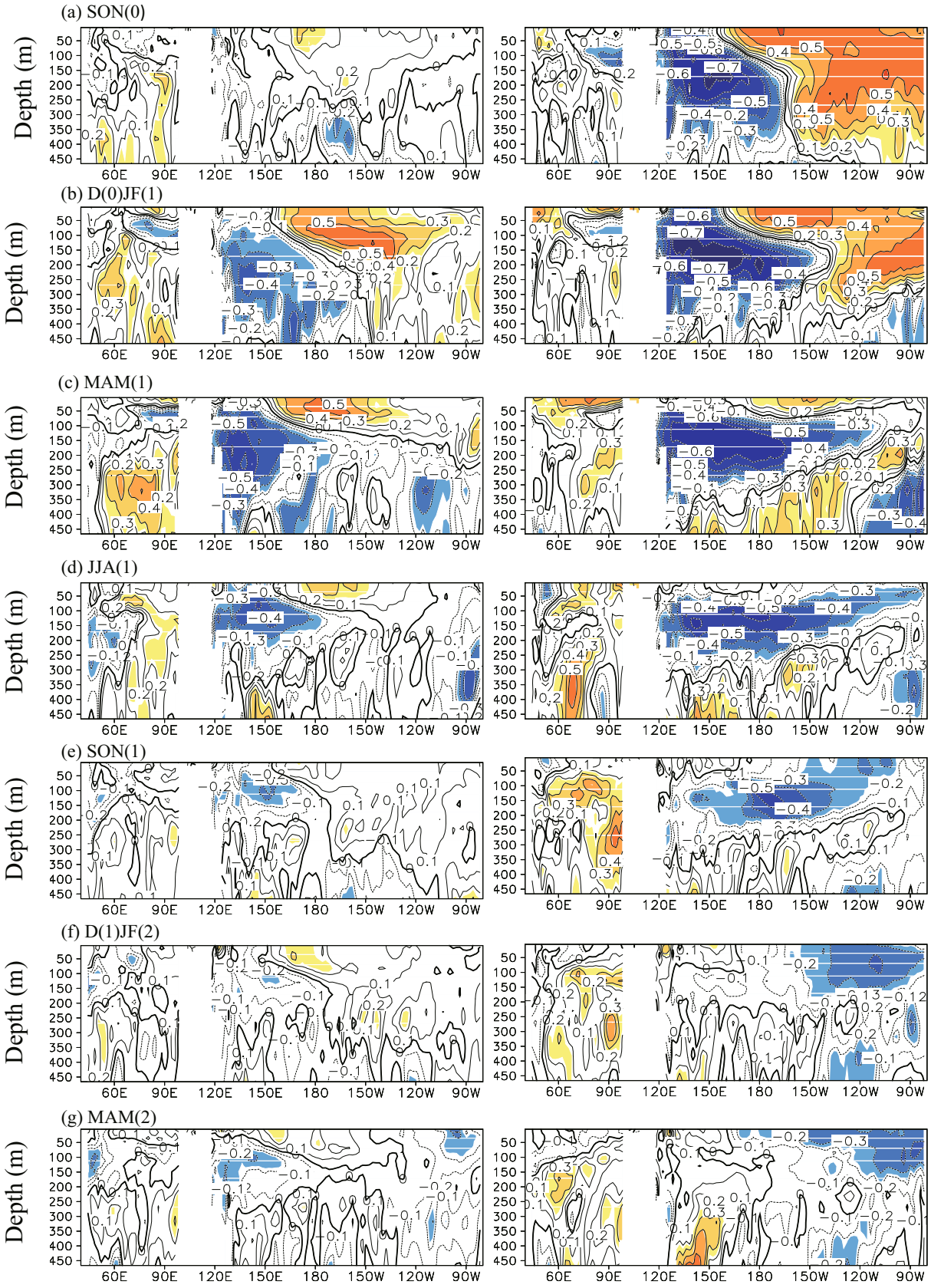

Fig. 8. Left-hand panels: lagged correlations between the ITF transport anomalies during the peak phase of the IOB (February to March) and subsurface temperature anomalies in the Indian–Pacific equatorial vertical section from the SODA data in different seasons. Right-hand panels: as in the left-hand panels, but for the ITF transport anomalies during the peak phase of the IOD (September to October). Color shading indicates positive and negative correlations above the 90% significance level.

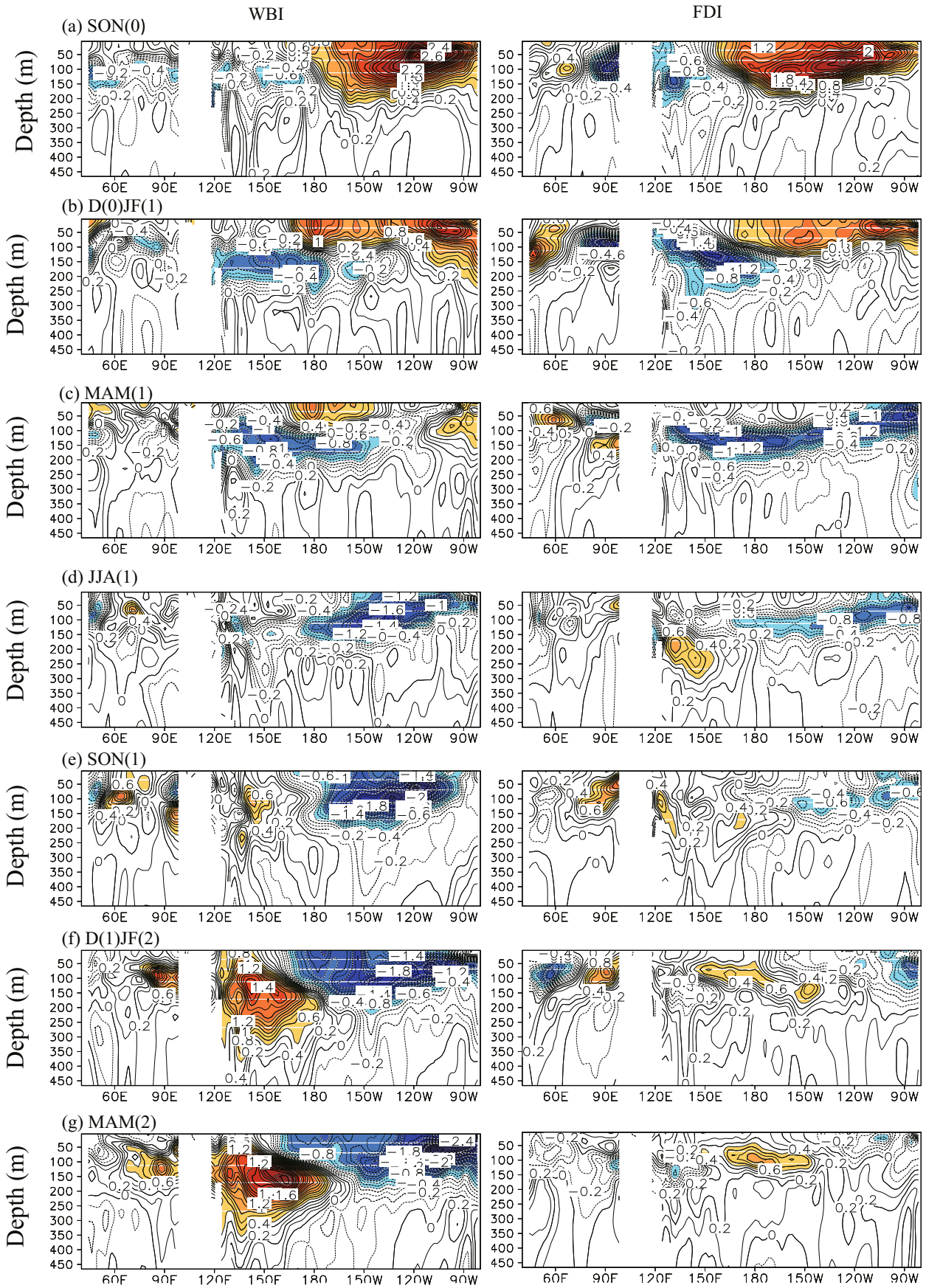

Fig. 9. As in Fig. 6, but with the influence of the ITF transport anomalies removed.

ponent significantly increases in the Indo-Pacific run, as compared to simulations only including Pacific coupling (e.g., Yu, 2005). Izumo et al. (2014) also indicated that the interactions between ENSO, the IOD and the IOB operate on a biennial timescale.

Many recent studies (e.g., Ohba and Ueda, 2009; Ohba et al., 2010; Okumura et al., 2011; Dommenget et al., 2013; Ohba, 2013) show that the transition process of ENSO is asymmetric. Ohba and Watanabe (2012) showed asymmetric impacts of the IOB on ENSO transition between the warming and cooling phase of ENSO. Moreover, it is found that the asymmetric impact on El Niño and La Niña also exist for the IOD when we separate the analysis for the positive and negative phase of the IOD. The details and relative roles of the atmospheric bridge and oceanic channel will be discussed in another paper.

The relationship between the tropical Indian Ocean SSTAs and ENSO transition is influenced by multiple factors. Many studies have documented interdecadal variability in ENSO or the Indian Ocean SSTAs. Izumo et al. (2014) explored the interdecadal robustness of the influence of the IOD and Pacific recharge on the following year's El Niño over the period 1872–2008, with a focus on the atmospheric bridge process. Yuan et al. (2013) concluded that the dynamics are not related to the atmospheric bridge over the period 1990–2009, which supports the ITF connection. Thus, the relative roles of the atmospheric bridge and oceanic channel may be different in this lagged remote relationship over different periods. In addition to the FDI, the 1-year lagged correlations of the WBI with the following year's ENSO also possess significant interdecadal variability (not shown). Therefore, the lagged relationship between the tropical Indian Ocean SSTAs and ENSO transition on interdecadal timescales, and the associated dynamical processes, still need further investigation. In addition, tropical Atlantic warming during El Niño is also clear, and some of the differences between the two Indian Ocean SSTAs modes might originate from the Atlantic SST variability. Therefore, the role of Atlantic SST variability in Indian Ocean SST variability needs further investigation.

Using a novel method based on information flow, Liang (2014) discussed the relationship between the IOD and ENSO. The study indicated that the IOD and ENSO are mutually causal, but the causality is asymmetric: the IOD functions to make ENSO more uncertain, while ENSO tends to stabilize the IOD. This new method has not been applied to investigate the influence of the IOB on ENSO. It would be of interest to discuss the relationship between the IOB and ENSO, including ENSO's phase transition.

5. Conclusion

The tropical Indian and Pacific oceans can affect one another. Rather than discussing whether or not ENSO triggers the SSTAs in the tropical Indian Ocean, the present paper focuses on the effects of the leading modes of the SSTAs in the tropical Indian Ocean on the variability of ENSO about 1 year later, which is not a synchronous influence. The SSTAs in the tropical Indian Ocean have two major modes: the IOB and IOD. Their occurrence influences the variation in the tropical Pacific Ocean.

However, the influence on ENSO transition associated with the IOB and IOD has previously only been examined in isolation and using data with different time periods. In particular, whilst IOD events are always followed by IOB events, previous studies have not considered the effect between these two modes. Moreover, the model experiment of Ohba and Ueda (2007) did not reproduce this significant connection between the IOD and the tropical central-eastern Pacific. The present study compares the relationship between the IOB/IOD and ENSO transition in the following year using observational data for 1958–2008, through partial correlation analysis and composite analysis to separate the effect between the preceding IOD and following IOB. Our results indicate that both the positive (negative) phase of the IOB and IOD (independent of each other) in the tropical Indian Ocean are possible contributors to the El Niño (La Niña) decay and phase transition to La Niña (El Niño) about 1 year later. The difference is that the influence induced by the IOB is stronger than that by the IOD.

The cold (warm) SSTAs in the equatorial central-eastern Pacific in the coming year originate from cold (warm) subsurface temperature anomalies in the equatorial eastern Indian and western Pacific Ocean. This signal propagates eastward and upward along the thermocline to arrive at the surface. Some studies have indicated that the generation and propagation of subsurface temperature anomalies might come from the modulation of the oceanic channel, in addition to the atmospheric bridge. However, for the IOB, previous studies only focused on the atmospheric bridge process, without discussion of the role of the oceanic channel process in the relationships with ENSO transition. Our results show that the relative contributions of the oceanic channel are different for the IOB and IOD. For the IOD, the Kelvin waves induced by the IOD could penetrate from the Indian Ocean into the western Pacific through the ITF, which further propagate eastward and upward to induce ENSO decay and transition in the following year. However, for the IOB, the associated Kelvin waves propagate to the equatorial western Pacific without propagation to the eastern Pacific, which disappear in the western Pacific during the coming summer–fall. The indication is that the ITF transport anomalies are ineffective as a link between the IOB signals and ENSO phase transition. However, why the Kelvin waves induced by the IOB are unable to propagate further to the eastern Pacific remains an open question.

Furthermore, it can be seen from Fig. 10 that the atmospheric bridge process plays a dominant role in the lagged teleconnection between the IOB and ENSO phase transition. For the IOB, significant easterly anomalies over the western Pacific occur during D(0)JF(1), which sustain to the following summer [JJA(1)]. Through the baroclinic atmosphere Kelvin wave, the IOB in the Indian Ocean can affect the development of the anomalous easterlies in the western Pacific (e.g., Xie et al., 2009; Du et al., 2013), which then influence

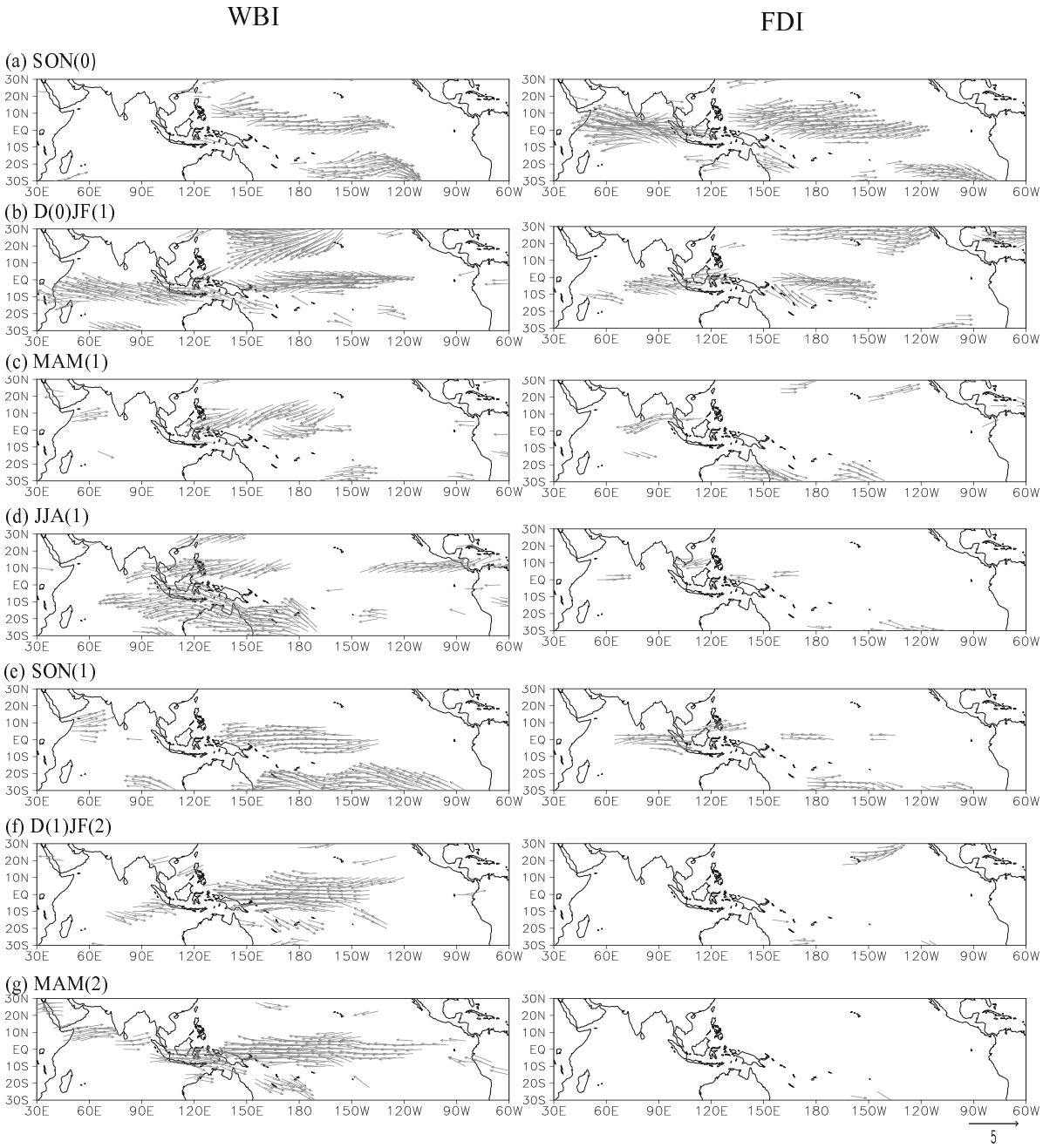

Fig. 10. Composites of tropical wind anomalies (m s^{-1}) at 850 hPa in different seasons for the difference between independent positive and negative IOB events (left-hand panels) and the difference between independent positive and negative IOD events (right-hand panels).

El Niño's transition. However, the easterly anomalies over the western Pacific associated with the IOD are very weak throughout. Thus, the effect of the IOD on ENSO transition through the atmospheric bridge is not dominant.

Acknowledgements. This work was jointly supported by the Strategic Priority Research Program of the Chinese Academy of Sciences (Grant No. XDA11010102), the NSFC (Grant Nos. 41375094 and 41406028), the "973" project (Grant No. 2012CB956000), and the NSFC–Shandong Joint Fund for Marine Science Research Centers (Grant No. U1406401). The latest version of ERSST, ERSST.v3b, is available at http://www.esrl.noaa.gov/psd/, and the HADISST data at http://www.metoffice.gov.uk/hadobs/index.html, without charge. The SODA data are freely available from http://iridl.ldeo.columbia.edu/SOURCES/.CARTON-GIESE/.SODA, and ECMWF ORAS4 from http://www.ecmwf.int/en/research/climate-reanalysis/ocean-reanalysis.

REFERENCES

Annamalai, H., S. Kida, and J. Hafner, 2010: Potential impact of the tropical Indian Ocean-Indonesian Seas on El Niño char-

acteristics. *J. Climate*, **23**, 3933–3952.

Annamalai, H., S. P. Xie, J. P. McCreary, and R. Murtugudde, 2005: Impact of Indian Ocean sea surface temperature on developing El Niño. *J. Climate*, **18**, 302–319.

Balmaseda, M. A., K. Mogensen, and A. Weaver, 2013: Evaluation of the ECMWF ocean reanalysis system ORAS4. *Quart. J. Roy. Meteor. Soc*, **139**, 1131–1161 .

Behera, S. K., and T. Yamagata, 2003: Influence of the Indian Ocean dipole on the southern oscillation. *J. Meteor. Soc. Japan*, **81**, 169–177.

Carton, J. A., and B. S. Giese, 2008: A reanalysis of ocean climate using Simple Ocean Data Assimilation (SODA). *Mon. Wea. Rev.*, **136**, 2999–3017.

Cohen, J., and P. Cohen, 1983: *Applied Multiple Regression/Correlation Analysis for the Behavioral Sciences*. Lawrence Erlbaum Associates, 545 pp.

Ding, R. Q., and J. P. Li, 2012: Influences of ENSO teleconnection on the persistence of sea surface temperature in the tropical Indian Ocean. *J. Climate*, **25**, 8177–8195, doi: 10.1175/JCLI-D-11-00739.1.

Dommenget, D., T. Bayr, and C. Frauen, 2013: Analysis of the non-linearity in the pattern and time evolution of El Niño Southern Oscillation. *Climate Dyn.*, **40**, 2825–2847.

Drushka, K., J. Sprintall, S. T. Gille, and I. Brodjonegoro, 2010: Vertical structure of Kelvin waves in the Indonesian Throughflow exit passages. *J. Phys. Oceanogr.*, **40**, 1965–1987.

Du, Y., S.-P. Xie, Y.-L. Yang, X.-T. Zheng, L. Liu, and G. Huang, 2013: Indian Ocean variability in the CMIP5 multimodel ensemble: The basin mode. *J. Climate*, **26**, 7240–7266, doi: 10.1175/JCLI-D-12-00678.1.

England, M. H., and F. Huang, 2005: On the interannual variability of the Indonesian Throughflow and its linkage with ENSO. *J. Climate*, **18**, 1435–1444.

Izumo, T., and Coauthors, 2010: Influence of the state of the Indian Ocean Dipole on following year's El Niño. *Nature Geoscience*, **3**, 168–172

Izumo, T., M. Lengaigne, J. Vialard, J.-J. Luo, T. Yamagata, G. Madec, 2014: Influence of the Indian Ocean Dipole and Pacific recharge on the following year's El Niño: Interdecadal robustness. *Climate Dyn.*, **42**, 291–310, doi: 10.1007/s00382-012-1628-1.

Jin, F.-F., 1997a: An equatorial ocean recharge paradigm for ENSO. Part I: Conceptual model. *J. Atmos. Sci.*, **54**, 811–829.

Jin, F.-F., 1997b: An equatorial ocean recharge paradigm for ENSO. Part II: A stripped-down coupled model. *J. Atmos. Sci.*, **54**, 830–847.

Kandaga, P., A. L. Gordon, J. Sprintall, and R. D. Susanto, 2009: Intraseasonal variability in the Makassar Strait thermocline. *J. Mar. Res.*, **67**, 757–777.

Klein, S. A., B. J. Soden, and N.- C. Lau, 1999: Remote sea surface temperature variations during ENSO: Evidence for a tropical atmospheric bridge. *J. Climate*, **12**, 917–932.

Kug, J.-S., and I.-S. Kang, 2006: Interactive feedback between ENSO and the Indian Ocean. *J. Climate*, **19**, 1784–1801.

Kug, J.-S., T. Li, S.-I. An, I.-S. Kang, J.-J. Luo, S. Masson, and T. Yamagata, 2006: Role of the ENSO-Indian Ocean coupling on ENSO variability in a coupled GCM. *Geophys. Res. Lett.*, **33**, L09710, doi: 10.1029/2005GL024916.

Liang, X. S., 2014: Unraveling the cause-effect relation between time series. *Physical Review E*, **90**, 052150.

Luo, J.-J., R. C. Zhang, S. K. Behera, Y. Masumoto, F.-F. Jin, R. Lukas, and T. Yamagata, 2010: Interaction between El Niño and extreme Indian Ocean Dipole. *J. Climate*, **23**, 726–742.

McPhaden, M. J., 2008: Evolution of the 2006-2007 El Niño: The role of intraseasonal to interannual time scale dynamics. *Advances in Geosciences*, **14**, 219–230.

Mogensen, K., M. Alonso Balmaseda, and A. Weaver, 2012: The NEMOVAR ocean data assimilation system as implemented in the ECMWF ocean analysis for System 4. ECMWF Technical Memorandum 668, 59 pp.

Ohba, M., 2013: Important factors for long-term change in ENSO transitivity. *International Journal of Climatology*, **33**, 1495–1509.

Ohba, M., and H. Ueda, 2005: Basin-wide warming in the equatorial Indian Ocean associated with El Niño. *SOLA*, **1**, 89–92, doi: 10.2151/sola.2005-024.

Ohba, M., and H. Ueda, 2007: An impact of SST anomalies in the Indian Ocean in acceleration of the El Niño to La Niña transition. *J. Meteor. Soc. Japan*, **85**, 335–348.

Ohba, M., and H. Ueda, 2009: Role of nonlinear atmospheric response to SST on the asymmetric transition process of ENSO. *J. Climate*, **22**, 177–192.

Ohba, M., and M. Watanabe, 2012: Role of the Indo-Pacific interbasin coupling in predicting asymmetric ENSO transition and duration. *J. Climate*, **25**, 3321–3335.

Ohba, M., D. Nohara, and H. Ueda, 2010: Simulation of asymmetric ENSO transition in WCRP CMIP3 multimodel experiments. *J. Climate*, **23**, 6051–6067, doi: 10.1175/2010 JCLI3608.1.

Okumura, Y. M., M. Ohba, C. Deser, and H. Ueda, 2011: A proposed mechanism for the asymmetric duration of El Niño and La Niña. *J. Climate*, **24**, 3822–3829.

Potemra, J. T., 2005: Indonesian Throughflow transport variability estimated from satellite altimetry. *Oceanography*, **18**, 98–107.

Rayner, N. A., D. E. Parker, E. B. Horton, C. K. Folland, L. V. Alexander, D. P. Rowell, E. C. Kent, and A. Kaplan, 2003: Global analyses of sea surface temperature, sea ice, and night marine air temperature since the late nineteenth century. *J. Geophys. Res.*, **108** , 4407, doi: 10.1029/2002JD002670.

Saji, N. H., and T. Yamagata, 2003: Structure of SST and surface wind variability during Indian Ocean dipole mode events: COADS observations. *J. Climate*, **16**, 2735–2751.

Saji, N. H., B. N. Goswami, P. N. Vinayachandran, and T. Yamagata, 1999: A dipole mode in the tropical Indian Ocean. *Nature*, **401**, 360–363.

Smith, T. M., R. W. Reynolds, T. C. Peterson, and J. Lawrimore, 2008: Improvements to NOAA's historical merged land-ocean surface temperature analysis (1880–2006). *J. Climate*, **21**, 2283–2296.

Sprintall, J., A. L. Gordon, R. Murtugudde, and R. D. Susanto, 2000: A semiannual Indian Ocean forced Kelvin wave observed in the Indonesian seas in May 1997. *J. Geophys. Res.*, **105**, 17 217–17 230.

Suarez, M. J., and P. S. Schopf, 1988: A delayed action oscillator for ENSO. *J. Atmos. Sci.*, **45**, 3283–3287.

Tillinger, D., and A. L. Gordon, 2009: Fifty years of the Indonesian Throughflow. *J. Climate*, **22**, 6342–6355.

Wajsowicz, R. C., and E. K. Schneider, 2001: The Indonesian throughflow's effect on global climate determined from the COLA coupled climate system. *J. Climate*, **14**, 3029–3042.

Webster, P. J., A. M. Moore, J. P. Loschnigg, and R. R.. Leben, 1999: Coupled ocean-atmosphere dynamics in the Indian Ocean during 1997–98. *Nature*, **401**, 356–360.

Weisberg, R. H., and C. Z. Wang, 1997: A western Pacific oscillator paradigm for the El Niño-Southern Oscillation. *Geophys. Res. Lett.*, **24**, 779–782.

Wijffels, S. E., and G. Meyers, 2004: An intersection of oceanic waveguides: Variability in the Indonesian Throughflow region. *J. Phys. Oceanogr.*, **34**, 1232–1253.

Wu, R. G., and B. P. Kirtman, 2004: Understanding the impacts of the Indian Ocean on ENSO variability in a coupled GCM. *J. Climate*, **17**, 4019–4031.

Wyrtki, K., 1987: Indonesian through flow and the associated pressure gradient. *J. Geophys. Res.*, **92**, 12 941–12 946.

Xie, S.-P., H. Annamalai, F. A. Schott, and J. P. McCreary Jr, 2002: Structure and mechanisms of South Indian Ocean climate variability. *J. Climate*, **15**, 864–878.

Xie, S.-P., K. M. Hu, J. Hafner, H. Tokinaga, Y. Du, G. Huang, and T. Sampe, 2009: Indian Ocean capacitor effect on Indo-western Pacific climate during the summer following El Niño. *J. Climate*, **22**, 730–747.

Xue, Y., T. M. Smith, and R. W. Reynolds, 2003: Interdecadal changes of 30- yr SST normals during 1871–2000. *J. Climate*, **16**, 1601–1612.

Yamagata, T., S. K. Behera, S. A. Rao, Z. Y. Guan, K. Ashok, and H. N. Saji, 2003: Comments on "Dipoles, temperature gradients, and tropical climate anomalies". *Bull. Amer. Meteor. Soc.*, **84**, 1418–1422.

Yang, J. L., Q. Y. Liu, S.-P. Xie, Z. Y. Liu, and L. X. Wu, 2007: Impact of the Indian Ocean SST basin mode on the Asian summer monsoon. *Geophys. Res. Lett.*, **34**, L02708, doi: 10.1029/2006GL028571.

Yasunari, T., 1985: Zonally propagating modes of the global east–west circulation associated with the Southern Oscillation. *J. Meteor. Soc. Japan*, **63**, 1013–1029.

Yasunari, T., 1987: Global structure of the El Niño/Southern oscillation. Part II. Time evolution. *J. Meteor. Soc. Japan*, **65**, 81–102.

Yu, J.-Y., C. R. Mechoso, J. C. McWilliams, and A. Arakawa, 2002: Impacts of the Indian Ocean on the ENSO cycle. *Geophys. Res. Lett.*, **29**, 46-1–6-4, doi: 10.1029/2001GL014098.

Yu, J.-Y ., 2005: Enhancement of ENSO's persistence barrier by biennial variability in a coupled atmosphere-ocean general circulation model. *Geophys. Res. Lett.*, **32**, L13707, doi: 10.1029/2005GL023406.

Yu, W. D., B. Q. Xiang, L. Liu, and N. Liu, 2005: Understanding the origins of interannual thermocline variations in the tropical Indian Ocean. *Geophys. Res. Lett.*, **32**, L24706, doi: 10.1029/2005GL024327.

Yuan, D. L., and Coauthors , 2011: Forcing of the Indian Ocean dipole on the interannual variations of the tropical Pacific Ocean: Roles of the Indonesian throughflow. *J. Climate*, **24**, 3593–3608.

Yuan, D. L., H. Zhou, and X. Zhao, 2013: Interannual climate variability over the tropical Pacific Ocean induced by the Indian Ocean dipole through the Indonesian Throughflow. *J. Climate*, **26**, 2845–2861, doi: 10.1175/JCLI-D-12-00117.1.

Zhou, Q., W. S. Duan, M. Mu, and R. Feng, 2015: Influence of positive and negative Indian Ocean dipoles on ENSO via the Indonesian Throughflow: Results from sensitivity experiments. *Adv. Atmos. Sci.*, **32**, 783–793, doi: 10.1007/s00376-014-4141-0.